EJTP **5, No. 17** (2008) 111–124 *Electronic Journal of Theoretical Physics*

A Two-dimensional Discrete Mapping with C^∞ Multifold Chaotic Attractors

Zeraoulia Elhadj[a*], J. C. Sprott[b†]

[a] *Department of Mathematics, University of Tébéssa, (12000), Algeria.*
[b] *Department of Physics, University of Wisconsin, Madison, WI 53706, USA.*

Received 22 May 2007, Accepted 26 October 2007, Published 27 March 2008

Abstract: This paper introduces a two-dimensional, C^∞ discrete bounded map capable of generating "*multi- fold*" strange attractors via period-doubling bifurcation routes to chaos.

Keywords: C^∞ 2-D Chaotic map, Multifold Chaotic Attractors.
PACS (2006): 05.45.-a, 05.45.Gg.

1. Introduction

Discrete mathematical models are usually derived from theory or experimental observation, or as an approximation to the Poincaré section for some continuous-time models. Many papers have described chaotic systems, one of the most famous being a two-dimensional discrete map suggested by Hénon [3] and studied in detail by others [3,4,11,12]. It is possible to change the form of this map to obtain other chaotic attractors [5,6,7,8,14] or to make some C^1-modifications to obtain "*multifold*" strange chaotic attractors [6] with possible applications in secure communications because of their chaotic properties [9,10].

The Hénon map is a prototypical two-dimensional invertible iterated map with a chaotic attractor and is a simplified model of the Poincaré map for the Lorenz equation proposed by Hénon in 1976 and given by:

$$H\left(x_n, y_n\right) = \begin{pmatrix} x_{n+1} \\ y_{n+1} \end{pmatrix} = \begin{pmatrix} 1 - ax_n^2 + by_n \\ x_n \end{pmatrix} \tag{1}$$

* zeraoulia@mail.univ-tebessa.dz and zelhadj12@yahoo.fr
† sprott@physics.wisc.edu

For $b = 0$, the Hénon map reduces to the quadratic map [1], which is conjugate to the logistic map. Bounded solutions exist for the Hénon map over a range of a and b values, and a portion of this range yields chaotic attractors.The Hénon procedure permits the construction of a family of attractors dependent on the two parameters a and b, but it does not have attractors with "*multifolds*." However, appropriate C^1-modifications can result in such attractors [6].

In this paper we study a modified Hénon map given by:

$$f(x_n, y_n) = \begin{pmatrix} x_{n+1} \\ y_{n+1} \end{pmatrix} = \begin{pmatrix} 1 - a\sin x_n + by_n \\ x_n \end{pmatrix}, \tag{2}$$

or equivalently:

$$x_{n+1} = 1 - a\sin x_n + bx_{n-1}. \tag{3}$$

where the quadratic term x^2 in the Hénon map is replaced by the nonlinear term $\sin x$, and we study this model for all values of a and b. The essential motivation for this work is to develop a C^∞ mapping that is capable of generating chaotic attractors with "*multifolds*" via a period-doubling bifurcation route to chaos which has not been studied before in the literature. The fact that this map is C^∞ in some ways simplifies the study of the map and avoids some problems related to the lack of continuity or differentiability of the map. The choice of the term $\sin x$ has an important role in that it makes the solutions bounded for values of b such that $|b| \leq 1$, and all values of a, while they are unbounded for $|b| > 1$. On the other hand, this is not the only possible choice, for example one can use the term $\cos x$.

2. Analytical results

In all proofs given here, we use the following standard results:

Theorem 1. *Let* $(x_n)_n$, *and* $(z_n)_n$ *be two real sequences, if* $|x_n| \leq |z_n|$ *and* $\lim_{n\longrightarrow+\infty} |z_n| = A < +\infty$, then $\lim_{n\longrightarrow+\infty} |x_n| \leq A$, or *if* $|z_n| \leq |x_n|$, *and* $\lim_{n\longrightarrow+\infty} |z_n| = +\infty$ *then,* $\lim_{n\longrightarrow+\infty} |x_n| = +\infty$.

The proof of this result is available in standard mathematics books and will not be given here.

We use this result to construct a sequence $(z_n)_n$ that satisfies the above conditions for determining whether the difference equation (3) has bounded or unbounded orbits.

Theorem 2. *For all values of* a *and* b *the sequence* $(x_n)_n$ given in (3) *satisfies the following inequality:*

$$|1 - x_n + bx_{n-2}| \leq |a|, \tag{4}$$

Proof. We have for every $n > 1$: $x_n = 1 - a \sin x_{n-1} + b x_{n-2}$, then, one has:

$$|-x_n + 1 + b x_{n-2}| = |a \sin x_{n-1}| \leq |a|, \tag{5}$$

since $\sup_{x \in \mathbb{R}} |\sin x| = 1$.

Theorem 3. F*or every* $n > 1$*, and all values of* a *and* b*, and for all values of the initial conditions* $(x_0,\ x_1) \in \mathbb{R}^2$*, the sequence* $(x_n)_n$ *satisfies the following equalities:*

(a) *If* $b \neq 1$, then:

$$x_n = \begin{cases} \frac{b^{\frac{n-1}{2}} - 1}{b-1} + b^{\frac{n-1}{2}} x_1 - a \sum\limits_{p=1}^{p=\frac{n-1}{2}} b^{p-1} \sin x_{n-(2p-1)}, \text{ if } n \text{ is odd}, \\ \frac{b^{\frac{n}{2}} - 1}{b-1} + b^{\frac{n}{2}} x_0 - a \sum\limits_{p=1}^{p=\frac{n}{2}} b^{p-1} \sin x_{n-(2p-1)}, \text{ if } n \text{ is even}, \end{cases} \tag{6}$$

(b) If $b = 1$, then:

$$x_n = \begin{cases} \frac{n-1}{2} + x_1 - a \sum\limits_{p=1}^{p=\frac{n-1}{2}} \sin x_{n-(2p-1)}, \text{ if } n \text{ is odd} \\ \frac{n}{2} + x_0 - a \sum\limits_{p=1}^{p=\frac{n}{2}} \sin x_{n-(2p-1)}, \text{ if } n \text{ is even} \end{cases} \tag{7}$$

Proof. Assume that n is odd, then we have for every $n > 1$, the following equalities:

$$x_n = 1 - a \sin x_{n-1} + b x_{n-2}, \tag{8}$$

$$x_{n-2} = 1 - a \sin x_{n-3} + b x_{n-4}, \tag{9}$$

$$x_{n-4} = 1 - a \sin x_{n-5} + b x_{n-6} ... \tag{10}$$

Then the results in (6) and (7) are obtained by successive substitutions of (9), (10),... into (8) for all $k = n-2, n-4, ..., 2$. The other cases can be obtained using the same logic.

Theorem 4. *The fixed points* (l, l) *of the map (3) exist if one of the following conditions holds:*

(i) If $a \neq 0$*, and* $b \neq 1$*, then* l *satisfies the following conditions:*

$$\begin{cases} 1 - a \sin l + (b-1)\, l = 0, \text{ and } l \leq \frac{1+|a|}{1-b}, \text{ if } b > 1, \\ \frac{1+|a|}{1-b} \leq l, \text{ if } b < 1, \end{cases} \tag{11}$$

(ii) If $b = 1$*, and* $|a| \geq 1$*, then,* l *is given by :* $l = \arcsin\left(\frac{1}{a}\right)$.
(iii) If $b \neq 1$*, and* $a = 0$ *, then,* l *is given by* $l = \frac{1}{1-b}$.
(iv) If $a = 0$*, and* $b = 1$*, there are no fixed points for the map (3).*

Proof. The proof is direct except for the case (i) where we apply Theorem 2, and

therefore one concludes that all fixed points of the map (3) are confined to the interval $\left]-\infty, \frac{1+|a|}{1-b}\right]$ if $b > 1$, and to $\left[\frac{1+|a|}{1-b}, +\infty\right[$ if $b < 1$. On the other hand, case (iii) gives a simple linear second-order difference equation $x_n = 1 + bx_{n-2}$, for which the situation is standard.

Since the location of the fixed points for map (3) cannot be calculated analytically, their stability will be studied numerically.

2.1 Existence of bounded orbits

In this subsection, we determine sufficient conditions for the map (3) to have bounded solutions. This is the interesting case since it includes the periodic, quasi-periodic, and chaotic orbits. First we prove the following theorem:

Theorem 5. *The orbits of the map (3) are bounded for all* $a \in \mathbb{R}$, *and* $|b| < 1$, *and all initial conditions* $(x_0, x_1) \in \mathbb{R}^2$.

Proof. From equation (3) and the fact that $\sin x$ is a bounded function for all $x \in \mathbb{R}$, one has the followings inequalities for all $n > 1$:

$$|x_n| \leq 1 + |a| + |bx_{n-2}|, \tag{12}$$

$$|x_{n-2}| \leq 1 + |a| + |bx_{n-4}|, \tag{13}$$

$$.... |x_{n-4}| \leq 1 + |a| + |bx_{n-2}|. \tag{14}$$

This implies from (12), (13), (14), ... that:

$$|x_n| \leq 1 + |a| + |bx_{n-2}|, \tag{15}$$

$$|x_n| \leq (1 + |a|) + |b| (1 + |a| + |bx_{n-4}|), \tag{16}$$

$$|x_n| \leq (1 + |a|) + (1 + |a|) |b| + |b|^2 |x_{n-4}|, ... \tag{17}$$

Hence, from (13) and (17) one has:

$$|x_n| \leq (1 + |a|) + (1 + |a|) |b| + |b|^2 (1 + |a|) + |b|^3 |x_{n-6}|, ... \tag{18}$$

Since $|b| < 1$, then the use of (18) and induction about some integer k using the sum of a geometric growth formula permits us to obtain the following inequalities for every $n > 1, k \geq 0$:

$$|x_n| \leq (1 + |a|) \left(\frac{1 - |b|^k}{1 - |b|}\right) + |b|^k |x_{n-2k}|. \tag{19}$$

where k is the biggest integer j such that $j \leq \frac{n}{2}$. Thus one has the following two cases:

(1) if n is odd, i.e. $\exists m \in \mathbb{N}$, such that $n = 2m + 1$, then the biggest integer $k \leq \frac{n}{2}$ is $k = \frac{n-1}{2}$, for which $(x_n)_n$ satisfies the following inequalities:

$$|x_{2m+1}| \leq (1 + |a|) \left(\frac{1 - |b|^m}{1 - |b|}\right) + |b|^m |x_1| = z_m, \tag{20}$$

(2) if n is even, i.e. $\exists m \in \mathbb{N}$, such that $n = 2m$, then, the biggest integer $k \leq \frac{n}{2}$ is $k = \frac{n}{2}$, for which x_n satisfies the following inequalities :

$$|x_{2m}| \leq (1 + |a|) \left(\frac{1 - |b|^m}{1 - |b|} \right) + |b|^m |x_0| = u_m, \tag{21}$$

Thus, since $|b| < 1$, the sequences $(z_m)_m$ and $(u_m)_m$ are bounded, and one has:

$$\begin{cases} z_m \leq \frac{(1+|a|)}{1-|b|} + \left| |x_1| - \frac{(1+|a|)}{1-|b|} \right|, \text{for all } m \in \mathbb{N}. \\ u_m \leq \frac{(1+|a|)}{1-|b|} + \left| |x_0| - \frac{(1+|a|)}{1-|b|} \right|, \text{for all } m \in \mathbb{N}. \end{cases} \tag{22}$$

Thus Formulas (20), (21), and inequalities (22) give the following bounds for the sequence $(x_n)_n$:

$$|x_n| \leq \max \left(\frac{(1 + |a|)}{1 - |b|} + \left| |x_0| - \frac{(1 + |a| \, \delta)}{1 - |b|} \right|, \frac{(1 + |a|)}{1 - |b|} + \left| |x_1| - \frac{(1 + |a|)}{1 - |b|} \right| \right). \tag{23}$$

Finally, for all values of a and all values of b satisfying $|b| < 1$ and all initial conditions $(x_0, x_1) \in \mathbb{R}^2$, one concludes that all orbits of the map (3) are bounded, i.e. in the subregion of $\mathbb{R}^4$:

$$\Omega_1 = \left\{ (a, b, x_0, x_1) \in \mathbb{R}^4 / \ |b| < 1 \right\}. \tag{24}$$

Hence the proof is completed.

2.2 Existence of unbounded orbits

In this subsection, we determine sufficient conditions for which the orbits of the map (3) are unbounded. First we prove the following theorem:

Theorem 6. The map (3) possesses unbounded orbits in the following subregions of $\mathbb{R}^4$:

$$\Omega_2 = \left\{ (a, b, x_0, x_1) \in \mathbb{R}^4 / \ |b| > 1, \text{ and both } |x_0|, |x_1| > \frac{|a| + 1}{|b| - 1} \right\}, \tag{25}$$

and

$$\Omega_3 = \left\{ (a, b, x_0, x_1) \in \mathbb{R}^4 / \ |b| = 1, \text{ and } |a| < 1 \right\}. \tag{26}$$

Proof. (a) For every $n > 1$, we have: $x_n = 1 - a \sin x_{n-1} + b x_{n-2}$. Then $|b x_{n-2} - a \sin x_{n-1}| =$

$|x_n - 1|$ and $||b x_{n-2}| - |a \sin x_{n-1}|| \leq |x_n - 1|$. (We use the inequalities: $|x| - |y| \leq ||x| - |y|| \leq |x - y|$). This implies that

$$|b x_{n-2}| - |a \sin x_{n-1}| \leq |x_n| + 1. \tag{27}$$

Since $|\sin x_{n-1}| \leq 1$, this implies $-|a \sin x_{n-1}| \geq -|a|$, and $|b x_{n-2}| - |a \sin x_{n-1}| \geq |b x_{n-2}| - |a|$. Finally, one has from (27) that:

$$|b x_{n-2}| - (|a| + 1) \leq |x_n|. \tag{28}$$

Then, by induction as in the previous section, one has:

$$|x_n| \geq \begin{cases} \left(\frac{-(|a|+1)}{|b|-1} + |x_1|\right)|b|^{\frac{n-1}{2}} + \frac{|a|+1}{|b|-1}, \text{ if } n \text{ is odd,} \\ \\ \left(\frac{-(|a|+1)}{|b|-1} + |x_0|\right)|b|^{\frac{n}{2}} + \frac{|a|+1}{|b|-1}, \text{ if } n \text{ is even.} \end{cases} \tag{29}$$

Thus, if $|b| > 1$, and both $|x_0|$, $|x_1| > \frac{|a|+1}{|b|-1}$), one has: $\lim_{n\longrightarrow+\infty} |x_n| = +\infty$.

(b) For $b = 1$, one has:

$$|x_n| \geq \begin{cases} (1-|a|)\left(\frac{n-1}{2}\right) + x_1, \text{ if } n \text{ is odd,} \\ \\ (1-|a|)\left(\frac{n}{2}\right) + x_0, \text{ if } n \text{ is even.} \end{cases} \tag{30}$$

Hence, if $|a| < 1$, then one has: $\lim_{n\longrightarrow+\infty} x_n = +\infty$.

For $b = -1$, one has from Theorem 3 the inequalities:

$$x_n \leq \begin{cases} -\left(\frac{n-1}{2}\right) + x_1 + \left|\sum_{p=1}^{p=\frac{n-1}{2}} a\ (-1)^{p-1} \sin x_{n-(2p-1)}\right|, \text{ if } n \text{ is odd,} \\ \\ -\left(\frac{n}{2}\right) + x_0 + \left|\sum_{p=1}^{p=\frac{n}{2}} a\ (-1)^{p-1} \sin x_{n-(2p-1)}\right|, \text{ if } n \text{ is even.} \end{cases} \tag{31}$$

Because $\left|a\ (-1)^{p-1} \sin x_{n-(2p-1)}\right| \leq |a|$, then one has:

$$x_n \leq \begin{cases} (|a|-1)\left(\frac{n-1}{2}\right) + x_1, \text{ if } n \text{ is odd,} \\ \\ (|a|-1)\left(\frac{n}{2}\right) + x_0, \text{ if } n \text{ is even,} \end{cases} \tag{32}$$

Thus, if $|a| < 1$, then one has: $\lim_{n\longrightarrow+\infty} x_n = -\infty$.

Note that there is no similar proof for the following subregions of $\mathbb{R}^4$:

$$\Omega_4 = \left\{(a,b,x_0,x_1) \in \mathbb{R}^4 \ / \ |b| > 1, \text{and both } |x_0|, |x_1| \leq \frac{|a|+1}{|b|-1}\right\}, \tag{33}$$

$$\Omega_5 = \left\{(a,b,x_0,x_1) \in \mathbb{R}^4 \ / \ |b| = 1, \text{and } |a| \geq 1\right\}. \tag{34}$$

Hence, the proof is completed.

It can be easily seen from the above results that the Hénon-like map of the form (3) with a sine function may exhibit with respect to the parameter b the following behaviors:

(i) If $|b| < 1$, then the map (3) is bounded (See Theorem 5).

(ii) If $|b| \geq 1$, then the map (3) is unbounded (See Theorem 6).

3. Numerical simulations

3.1 Some observed mutifold attractors

In this section we present some observed mutifold chaotic attractors obtained by an appropriate choice of the parameters a and b. All the phase portraits presented in this paper are done in the xy-plane. We observe that the chaotic attractors evolve around a large number of fixed points, and it appears that the number of these points increase with increasing a when b is fixed.

There are several possible ways for a discrete dynamical system to transition from regular behavior to chaos. Bifurcation diagrams display these routes and allow one to identify the chaotic regions in ab-space from which the chaotic attractors can be determined. In this subsection we will illustrate some observed chaotic attractors, along with some other dynamical phenomena.

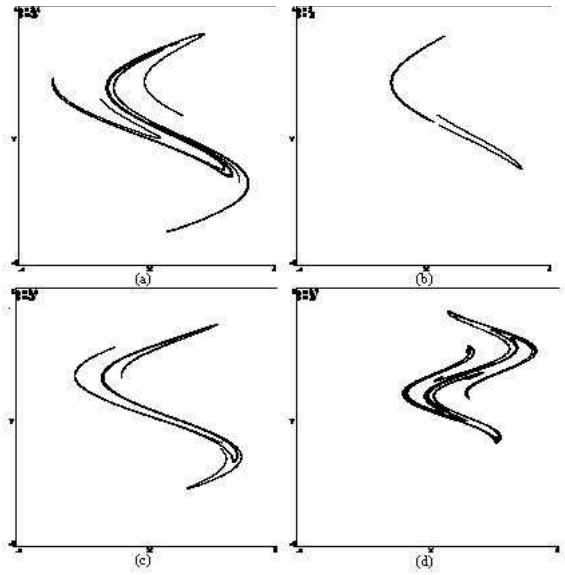

Fig. 1 Chaotic multifold attractors of the map (3) obtained for (a) $a = 2.4, b = -0.5$. (b) $a = 2, b = 0.2$. (c) $a = 2.8, b = 0.3$. (d) $a = 2.7, b = 0.6$.

3.2 Route to Chaos

It is well known that the Hénon map [3] typically undergoes a period-doubling route to chaos as the parameters are varied. By contrast, the Lozi map [8] has no period-doubling route, but rather it goes directly from a border-collision bifurcation developed from a stable periodic orbit [5]. Similarly, the chaotic attractor given in [14] is obtained from a border-collision period-doubling bifurcation scenario. This scenario involves a sequence of pairs of bifurcations, whereby each pair consists of a border-collision bifurcation and a pitchfork bifurcation. The other map given in [13] is obtained from a quasi-periodic route to chaos. Thus, the four chaotic systems go via different and distinguishable routes to chaos. Furthermore, the *multifold* chaotic attractors presented in Fig. 1 are obtained

from the map (3) via a period-doubling bifurcation route to chaos as shown in Fig. 5 (a).

3.3 Dynamical behaviors with parameter variation

In this subsection, the dynamical behaviors of the map (3) are investigated numerically.

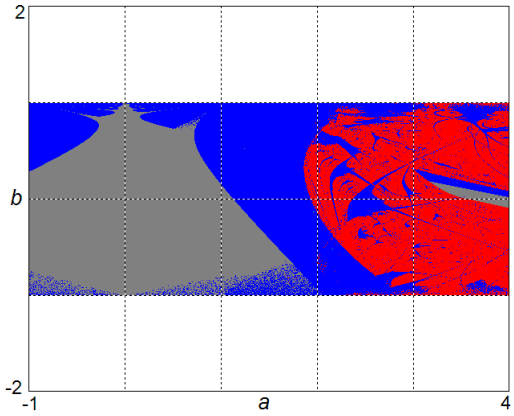

Fig. 2 Regions of dynamical behaviors in ab-space for the map (3).

Figure 2 shows regions of unbounded (white), fixed point (gray), periodic (blue), and chaotic (red) solutions in the ab-plane for the map (3), where we use 10^6 iterations for each point. On the other hand, if we fix parameter $b = 0.3$ and vary $-1 \leq a \leq 4$, the map (3) exhibits the dynamical behaviors as shown in Fig. 5.

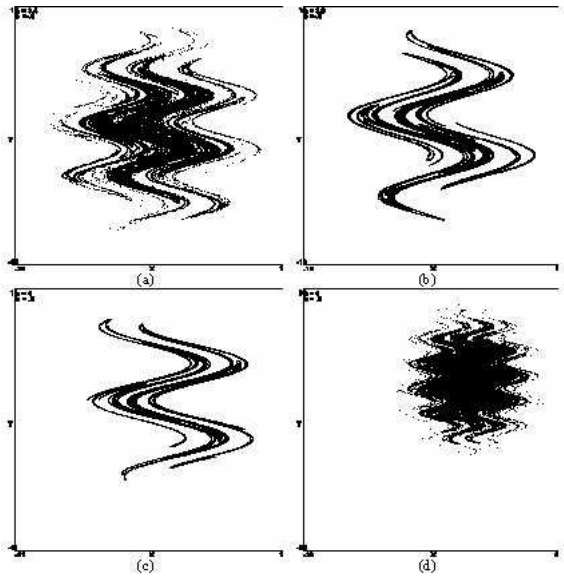

Fig. 3 Chaotic multifold attractors of the map (3) obtained for (a) $a = 3.4, b = -0.8$. (b) $a = 3.6, b = -0.8$. (c) $a = 4, b = 0.5$. (d) $a = 4, b = 0.9$.

In the interval $-1 \leq a \leq 0.76$, the map (3) converges to a fixed point. For $0.76 < a \leq 1.86$, there is a series of period-doubling bifurcations as shown in Fig. 5 (a). In the interval $1.86 < a \leq 2.16$, the orbit converges to a chaotic attractor. For $2.16 < a \leq 2.27$, it converges to a fixed point. For $2.27 < a \leq 2.39$, there are periodic windows. For

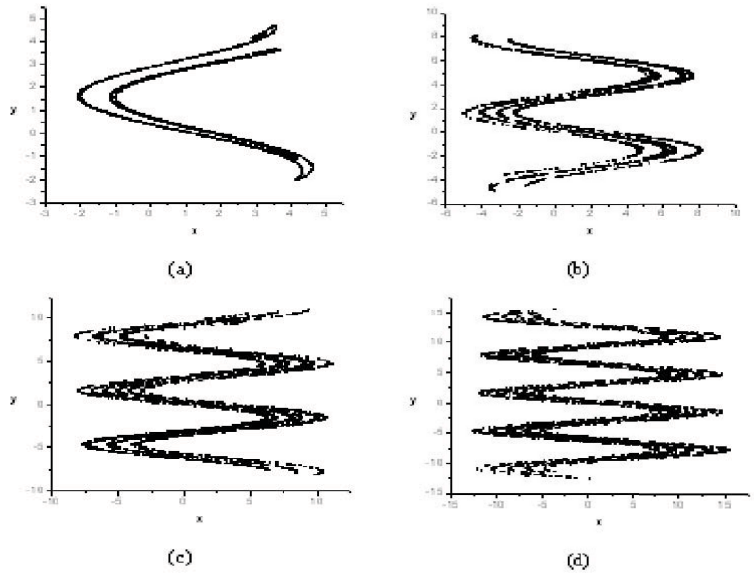

Fig. 4 Multifold chaotic attractors of the map (3) obtained for $b = 0.3$ and (a) $a = 3$. (b) $a = 5$. (c) $a = 7$. (d) $a = 10$.

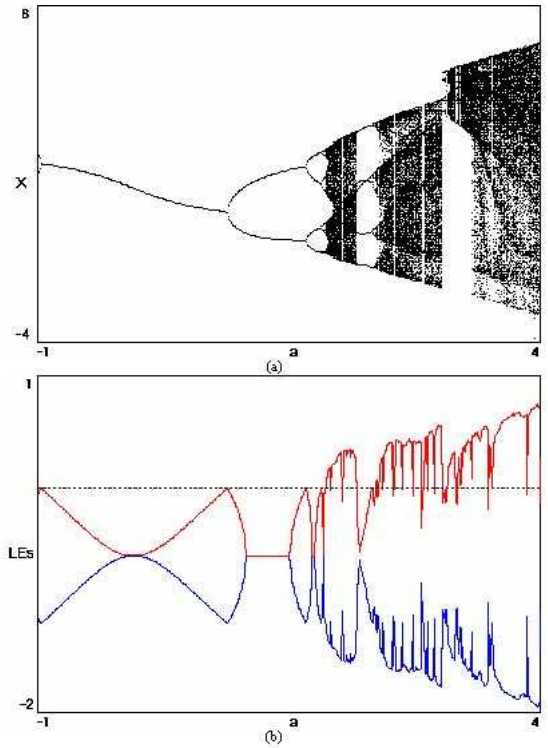

Fig. 5 (a) Bifurcation diagram for the map (3) obtained for $b = 0.3$ and $-1 \leq a \leq 4$. (b) Variation of the Lyapunov exponents of map (3) over the same range of a

$2.39 < a \leq 2.92$, it converges to a chaotic attractor. For $a > 2.92$, the map (3) is chaotic. For example, the Lyapunov exponents for $a = 3$ and $b = 0.3$ are $\lambda_1 = 0.56186$ and $\lambda_2 = -1.76583$, giving a Kaplan-Yorke dimension of $D_{KY} = 1.31818$. There are also fixed points and periodic orbits. This map is invertible for all $b \neq 0$, especially for $|b| < 1$,

and there is no hyperchaos since the sum of the Lyapunov exponents $\lambda_1 + \lambda_2 = \ln|b|$ is never positive. Generally, if we fix $b = 0.3$ and $-150 \leq a \leq 200$, map (3) is chaotic over all the range as shown in Fig. 6, except for the small intervals mentioned above and shown in Fig. 5.

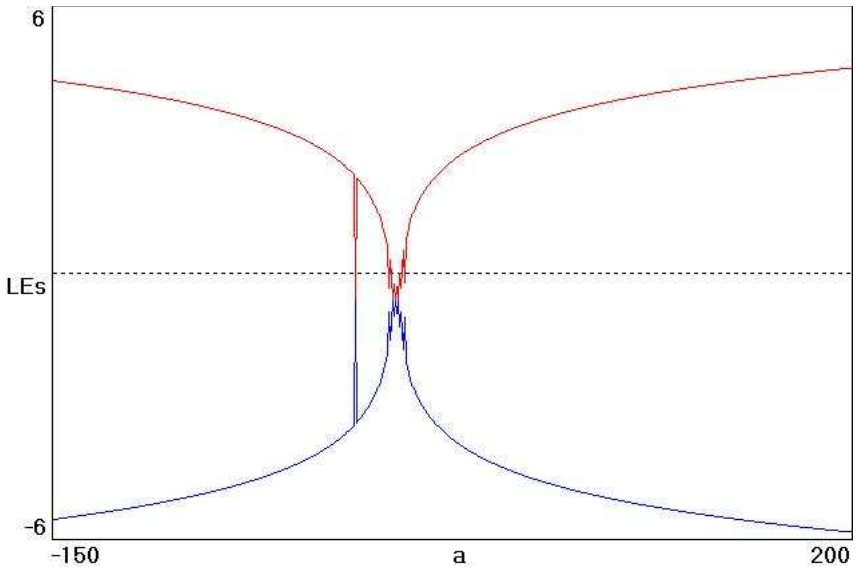

Fig. 6 Variation of the Lyapunov exponents of map (3) over the range $-150 \leq a \leq 200$ with $b = 0.3$.

However, if we fix parameter $a = 3$ and vary $b \in \mathbb{R}$, the map (3) exhibits very complicated dynamical behaviors as shown in Fig. 7, which shows some fixed points and some periodic windows. However, a large fraction of the region has chaotic attractors. Finally, for $|b| > 1$, the map (3) does not converge as shown in the previous section analytically.

For the map (3) we have calculated the attractors on a grid in ab-space (for $-1 \leq a \leq 4$) where the system is chaotic. There is a very wide variety of possible multifold chaotic attractors with different numbers of folds, only some of which are shown in Figs. 1, 3, and 4. The plots for the attractors do not show basin boundaries because the basins for bounded orbits include the entire xy-plane for $|b| < 1$.

There are regions of ab-space where two coexisting attractors occur as shown in black in Fig. 8, both in the regular and chaotic regimes. For example, with $a = 2$ and $b = -0.6$, a two-cycle (1.314326, -0.584114) coexists with a period-3 strange attractor. Similarly, for $a = 2.2$ and $b = -0.36$, there is a strange attractor surrounded by a second period-3 strange attractor as shown in black in Fig. 9 with their corresponding basins of attraction shown in yellow and magenta, respectively.

Figure 8 was obtained by using 200 different random initial conditions and looking for cases where the distribution of the average value of x on the attractor is bimodal. Since there is no rigorous test for bimodality, this was done by sorting the 200 values of $< x >$ and then dividing them into two equal groups. The group with the smallest range of $< x >$ was assumed to represent one of the attractors, and a second attractor was assumed to exist if the largest gap in the values of those in the other group was twice the

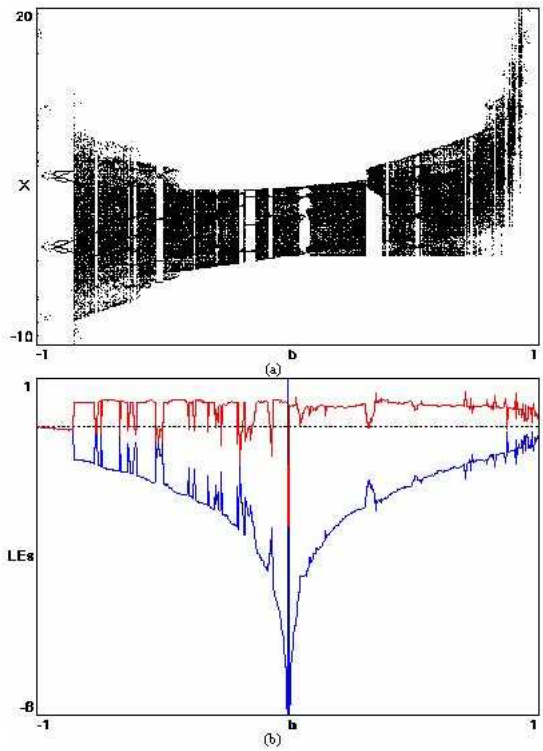

Fig. 7 a) Bifurcation diagram for the map (3) obtained for $a = 3$ and $-1 \leq b \leq 1$. (b) Variation of the Lyapunov exponents of map (3) for the same range of b.

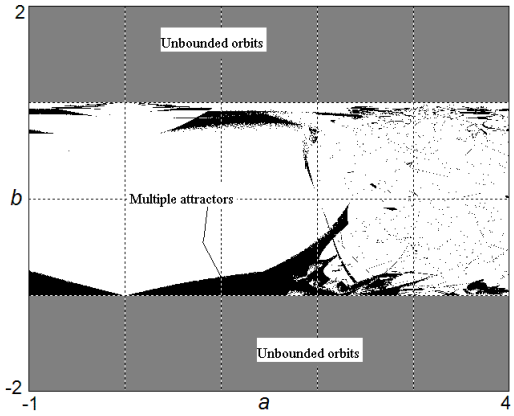

Fig. 8 The regions of ab-space where multiple attractors are found (shown in black).

range of the first group. The coexisting attractors where then confirmed in a separate calculation.

Conclusion

This paper reported the results of a detailed study of a C^∞ two-dimensional discrete map capable of generating smooth multifold strange attractors via period-doubling bifurcations.

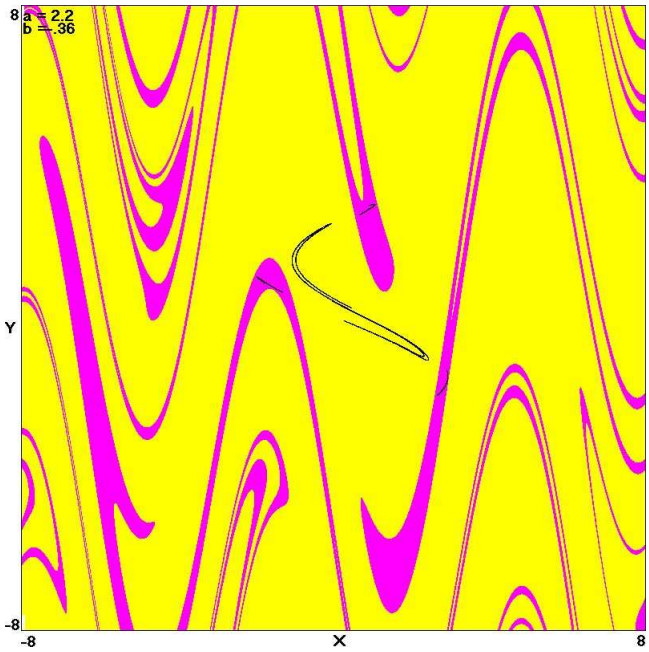

Fig. 9 Two coexisting attractors occur for $a = 2.2$ and $b = -0.36$, where a strange attractor is surrounded by a second period-3 strange attractor with their corresponding basins of attraction shown in yellow and magenta, respectively.

References

[1] M. Feigenbaum, The Universal Metric Properties of Nonlinear Transformation, *Journal of Stat. Phys.*, **21**, 669–706, (1979).

[2] Tsonis, Anastasios A., Chaos: From Theory to Applications, Plenum Press, New York, (1992).

[3] Hénon. M. , A two dimensional mapping with a stange attractor, *Commun. Math.P hys.*, **50**, (1976), 69–77, (1976).

[4] M. Benedicks and L. Carleson., The dynamics of the Hénon maps, *Ann. Math.*, **133**, 1–25, (1991).

[5] Cao. Y. and Liu. Z., Oriontation-preserving lozi map, *Chaos, Solitons & Fractals*, **9**, 11, 1857–1863, (1998).

[6] Aziz Alaoui M. A., MultiFold in a Lozi-type map. In preparation.

[7] Aziz Alaoui M. A., & C. Robert, & C. Grebogi., Dynamics of a Hénon-Lozi map, *Chaos, Solitons & Fractals*, **12** (11), 2323–2341, (2001).

[8] Lozi. R., Un attracteur étrange du type attracteur de Hénon, *Journal de Physique. Colloque* C5, Supplément au n^0 8, **39**, 9–10, (1978).

[9] Andreyev. Y. V. & Belsky. Y. L. & Dmitriev. A. S. & Kuminov. D. A., Information processing using dynamical chaos: Neural networks implentation, IEEE Transactions on Neural Networks, 7, 290–299, (1996).

[10] Newcomb. R. W. & Sathyan. S., An RC op amp chaos generator, *IEEE trans, Circuits & Systems*, **CAS-30**, 54–56, (1983).

[11] Sprott. J. C., Strange Attractors: Creating Patterns in Chaos, M &T Books, New York, (1993).

[12] Sprott. J. C., Chaos and Time-Series Analysis, Oxford University Press, (2003).

[13] Zeraoulia Elhadj, J. C. Sprott., A minimal 2-D quadratic map with quasi-periodic route to chaos. To appear in *Inter.J. Bifur & Chaos*, **18**(4) (2008).

[14] Zeraoulia Elhadj, A new chaotic attractor from 2-D discrete mapping via border-collision period doubling scenario, Discrete Dynamics in Nature and Society, Volume 2005, 235–238, (2005).